ELSEVIER

Journal of Photochemistry and Photobiology A: Chemistry 129 (1999) 9–15

Journal of Photochemistry and Photobiology A:Chemistry

www.elsevier.nl/locate/jphotochem

A resonance Raman study of Cl_2O photochemistry in solution: evidence for ClClO formation

A.P. Esposito [a], P.J. Reid [a,*], K.W. Rousslang [b]

[a] *Box 351700, Department of Chemistry, University of Washington, Seattle, WA 98195, USA*

[b] *Department of Chemistry, University of Puget Sound, 1500 Nth Warner, Tacoma, WA 98416, USA*

Received 22 June 1999; received in revised form 19 August 1999; accepted 19 August 1999

Abstract

The first resonance Raman spectra of Cl_2O dissolved in CCl_4 are reported. The dependence of the resonance Raman spectrum on incident energy is investigated and found to be consistent with the photochemical production of both ClO and ClClO. Both of these photoproducts appear linearly with incident energy at low power, but the scattering intensity of ClO is found to increase quadratically at higher energies. This behavior is proposed to be consistent with photodissociation of Cl_2O into ClO and Cl followed by partial geminate recombination of these fragments, resulting in ClClO formation. At higher excitation energies, photodissociation of ClClO is proposed to occur resulting in ClO production. Finally, the photochemical behavior of Cl_2O is compared to that of OClO, where geminate recombination does not result in formation of the analogous ClOO isomer. This comparison suggests that although geminate recombination is a characteristic feature of halo-oxide photochemistry in condensed environments, the products formed by recombination are species dependent.

Keywords: Resonance Raman; Halooxide photochemistry; ClOCl

1. Introduction

The importance of halo-oxides (Cl_xO_y and Br_xO_y) in both stratospheric and tropospheric chemistry has been recognized for some time. [1–4] These compounds can serve as halogen reservoir species, and may directly contribute to stratospheric ozone loss via photochemical decomposition resulting in atomic halogen formation. Interestingly, the photochemical behavior of halo-oxides is dependent on the environment. For example, photoexcitation of OClO results predominately in ClO and O production in the gas phase, but other processes such as Cl production, geminate recombination of the ClO and O photofragments, and photoisomerization to form ClOO become more prevalent in condensed environments [5]. In order to predict the environmental impact of halo-oxides, it is essential to understand why the photochemistry of these compounds is dependent on environment. Unraveling the phase dependence of halo-oxide reactivity represents a current challenge in physical-atmospheric chemistry.

Dichlorine monoxide (Cl_2O) is believed to play only a minor role in stratospheric chemistry [6–10]; however, it is the anhydrous form of hypochlorous acid (HOCl), a central chlorine reservoir species. [11,12] Although Cl_2O is not directly involved in atmospheric processes, comparative studies of halo-oxide photochemistry can serve to illustrate reactivity that is characteristic of this molecular class. For example, studies of OClO photochemistry have demonstrated that photodissociation to ClO and O in condensed environments is followed by rapid recombination of these fragments resulting in the reformation of OClO [13–20]. Low-temperature matrix isolation studies have demonstrated that ClOO is formed following OClO photoexcitation, but definitive evidence for the formation of this isomer in solution has yet to be reported [21–23]. Given this behavior, one might ask if geminate recombination and phase-dependent photoisomerization are representative of halo-oxide reactivity in general? The work presented here was performed to address this question.

In this manuscript, we present a resonance Raman study of Cl_2O photochemistry in solution. Extremely little is known about the solution-phase reactivity of Cl_2O. Although gas-phase and low-temperature matrix photochemistry of Cl_2O has been recently investigated [6–10,21,24–29], the

* Corresponding author.
E-mail address: preid@chem.washington.edu (P.J. Reid)

1010-6030/99/$ – see front matter
PII: S1010-6030(99)00181-1

solution-phase photochemistry of Cl_2O has not been investigated since the 1930s [30]. We present the first resonance Raman spectra of Cl_2O obtained with excitation at 282.4 nm, resonant with the $^1A_1$–$^1B_2$ and $^1A_1$–$^1B_1$ transitions of Cl_2O. A qualitative interpretation of the observed intensities suggests that upon photoexcitation, structural evolution occurs along all three normal coordinates. The power-dependence of the resonance Raman intensities is used to investigate photoproduct formation. We find that the production of ClClO is linearly dependent on excitation energy, and that the ClO appears quadratically with actinic energy at high incident power. A photochemical model consistent with this behavior is presented, where photoexcitation of Cl_2O results in ClO and Cl formation, with partial geminate recombination of these fragments resulting in the production of ClClO. Photoexcitation of ClClO at higher actinic energies provides a second channel for ClO formation. The possibility that ClClO may be formed by direct photoisomerization of Cl_2O is also discussed. The presence of ClClO in solution is contrasted with the behavior of OClO where geminate recombination of the primary photofragments results in the reformation of OClO. This comparison suggests that although geminate recombination may be a general feature of halo-oxide photochemistry in condensed environments, the products formed by geminate recombination will differ between members of this reaction class.

2. Experimental methods

2.1. Materials

Dichlorine monoxide (Cl_2O) was synthesized by two methods previously reported in the literature [31]. In the first method, Cl_2O dissolved in CCl_4 was prepared by passing chlorine gas (99.9%, Liquid Carbonic) through a 500-ml flask containing CCl_4 (99+% anhydrous, Aldrich) cooled to 0°C. Chlorine was added to the solvent until a concentration of 1.5 M was established as determined by vis-UV absorption [32]. Yellow mercuric oxide (J.T. Baker) was then added to the Cl_2 solution at a molar ratio of 1.1 HgO to Cl_2. The mixture was stirred for at least 45 min, with progress of the reaction evidenced by the formation of reddish brown Cl_2O. The mixture was strained through a sintered-glass filter to remove HgO. Sample purity and concentration were determined by vis-UV absorption. [32]. Typical Cl_2O concentrations of 0.50–0.70 M were obtained using this method.

In the second Cl_2O synthesis, yellow mercuric oxide was loosely packed in two glass columns (5 cm in diameter, 60 cm in length) containing glass beads. A mixture of 25% Cl_2 in N_2 (Airgas) was then passed sequentially through the columns. The presence of unreacted Cl_2 was checked by passing the gas exiting the columns over a small container containing ammonium hydroxide. The flow was reduced until the presence of white ammonium chloride was not observed, indicating the quantitative conversion of Cl_2 to Cl_2O. The resulting stream of Cl_2O was bubbled through CCl_4 cooled to 0°C. Typical Cl_2O concentrations obtained by this method were ∼0.10 M, with purity and concentration determined as described above. It should be noted that halo-oxides, in general, are highly oxidative, and that care must be taken when synthesizing and handling these compounds, since contact with reductive compounds can result in an explosion [33].

2.2. Resonance Raman spectra

Excitation at 282.4 nm was provided by the hydrogen-shifted second harmonic output of an Nd : YAG laser (Spectra-Physics GCR-170) operating at 30 Hz. The incident light was focused onto a thin-film, wire-guided jet of the Cl_2O solution using a 100-mm focal length, plano-convex, UV-quality spherical lens. Sample flow rates were sufficient to replace the illuminated sample volume between excitation pulses. A 135° backscattering geometry was employed with the scattered light collected and delivered to a 0.75-m spectrograph (Acton) using refractive, UV-quality optics. The scattered light passed through a polarization scrambler placed at the spectrograph entrance and was dispersed by a 2400-g/mm holographic grating. Entrance slit widths were adjusted to provide a spectral resolution of $\sim 8\,cm^{-1}$. The scattered light was detected with an 1100×300 pixel, back-thinned, liquid nitrogen-cooled CCD detector (Princeton Instruments). Resonance Raman spectra were corrected for the wavelength-dependent sensitivity of the spectrometer using a calibrated D_2 emission lamp (Hellma).

Photochemical studies were carried out by varying the excitation pulse energy and monitoring the resonance Raman intensities as a function of incident power (see below). Pulse energies were measured by a power meter (Scientech 365) equipped with a surface absorbing head, with measurements determined to have an accuracy of ±10%. Sample concentrations used in the experiments ranged from 0.04 to 0.30 M, with no concentration dependence evident for the results presented here. The Cl_2O concentrations were monitored at the start and end of a given experiment, with concentrations decreasing <30% over the course of an experiment due to evaporative loss of Cl_2O. Although the change in Cl_2O concentration is substantial, multichannel detection results in the integration of scattered intensity over all frequencies simultaneously, such that the relative intensities are insensitive to changes in concentration.

3. Results

3.1. Absorption

The electronic absorption spectrum of Cl_2O dissolved in carbon tetrachloride is presented in Fig. 1. Earlier studies

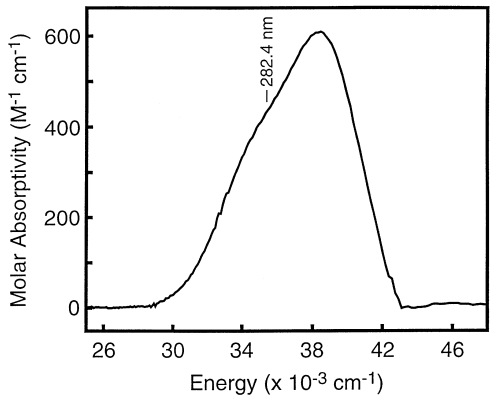

Fig. 1. Absorption spectrum of Cl_2O. Background due to the solvent (CCl_4) has been subtracted. Molar absorptivity values were taken from the literature [32]. The excitation wavelength at which the resonance Raman spectra were obtained is indicated.

have described the absorption intensity in this region as arising from two separate electronic transitions, with the bands located at 38 400 cm^{-1} (260 nm) and ~34 200 (292 nm) assigned to the $^1A_1 - {}^1B_2$ and $^1A_1 - {}^1B_1$ transitions, respectively [6,8,10]. Values for the molar-extinction coefficient of Cl_2O in carbon tetrachloride solution reported here are those provided in the literature [32]; however, it should be noted that published values for the molar absorptivity of gaseous Cl_2O are ~17% lower than those presented here [11,12,34].

3.2. Resonance Raman

The resonance Raman spectrum of Cl_2O obtained with an excitation energy of 27 μJ/pulse at 282.4 nm is presented in Fig. 2. Cl_2O fundamental transitions corresponding to the

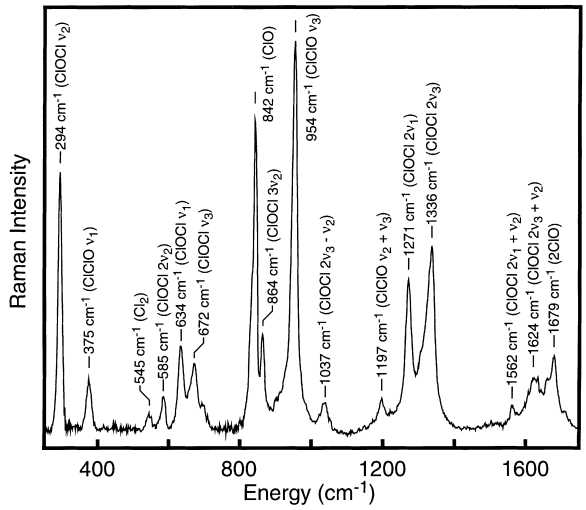

Fig. 2. Resonance Raman spectrum of Cl_2O in CCl_4 (180 mM) obtained with a pulse energy of 27 μJ at 282.4 nm. Scattering due to CCl_4 has been subtracted. Transitions corresponding to all three normal coordinates of Cl_2O are observed. In addition, scattering due to the ClO, Cl_2 and ClClO photoproducts is also observed.

symmetric stretch (ν_1), bend (ν_2), and asymmetric stretch (ν_3) modes are observed at 634, 294, and 672 cm^{-1}, respectively. These frequencies are in excellent agreement with previous Raman [28,35], infrared [21,27,29,33,36], and theoretical [37–40] studies. Substantial overtone and combination band intensity is observed for all three modes consistent with resonant enhancement. Interestingly, a difference transition corresponding to $2\nu_3 - \nu_2$ is observed at 1037 cm^{-1}, consistent with thermal excitation of the bend.

Resonance Raman intensities can be used to provide a mode-specific description of the excited-state potential energy surface. In particular, intensity in the resonance Raman spectrum demonstrates that the excited-state is displaced relative to the ground state along the corresponding normal coordinate. At first glance, all three modes of Cl_2O demonstrate intensity on resonance; therefore, excited-state structural evolution occurs along all three coordinates upon photoexcitation. However, a few observations temper this simple interpretation. First, the ground-state symmetry of ClOCl is $C_{2\nu}$ such that the asymmetric stretch coordinate is non-totally symmetric [41]. As such, intensity for the fundamental transitions on resonance is not expected; however, scattering along this coordinate is clearly observed. Substantial intensity for fundamental transitions involving non-totally symmetric coordinates has been observed for I_3^- and assigned to dynamical symmetry breaking in the excited-state by the solvent [42]. Dynamical symmetry breaking has also been suggested to be important in the photochemistry of OClO in CCl_4 [43]. Such an effect may also be operative in Cl_2O; however, further work is necessary to confirm this hypothesis. A second complication is that interpretation of the intensities as arising from resonance with a single electronic excited state is clearly erroneous. In addition, Fig. 1 demonstrates that the electronic transitions in this frequency region are relatively weak, such that pre-resonant contributions to the Raman intensities from states located further in the ultraviolet are to be expected. We are currently performing a complete resonance Raman intensity analysis of Cl_2O, and hope to clarify some of these issues in the near future. However, the focus of this work is to determine which photoproducts are formed following photoexcitation of Cl_2O, and the resonance Raman data presented here provide a detailed answer to this question.

In addition to Cl_2O, significant resonance Raman intensity is observed for various Cl_2O photoproducts. Resonance Raman intensity corresponding to ClO is observed at 842 cm^{-1}. Resonant enhancement of the ClO scattering is anticipated in that the absorption maximum of this species is 275 nm [44]. The frequency of the ClO stretch was reported to be 850 cm^{-1} by Chi and Andrews [28] in a matrix Raman photochemical study of Cl_2O. Infrared absorption studies of ^{35}ClO in the gas phase have reported values of 844 and 842 cm^{-1}, depending on the spin state observed [45,46]. Both studies support our assignment of the 842 cm^{-1} transition observed in Fig. 2 to ClO. Correspondingly, the transition at 1679 cm^{-1} is assigned to the first overtone of ClO.

In addition to ClO, scattering due to ClClO is also evident (Fig. 2). Since the excitation wavelength employed here is resonant with the electronic absorption spectrum of ClClO ($\lambda_{max} = 260$ nm), resonance enhancement of ClClO Raman scattering is expected [27,39]. We assign the transition at 375 cm^{-1} to the Cl–Cl stretch (ν_1), and the transition at 954 cm^{-1} to the Cl–O stretch (ν_3), in agreement with previous photochemical studies of matrix isolated Cl_2O [21,27,28]. The bending mode of ClClO (ν_2) has a frequency of 240–241 cm^{-1} [27,28], and although the region <250 cm^{-1} was not studied, a transition at 1197 cm^{-1} corresponds to the $\nu_2 + \nu_3$ ClClO combination band consistent with this frequency assignment. To our knowledge, *the data presented in Fig. 2 represent the first spectroscopic evidence of the production of ClClO in solution following photoexcitation of Cl_2O.*

Finally, resonance Raman scattering from Cl_2 is observed at 545 cm^{-1}. This frequency is in good agreement with the value of 548 cm^{-1} reported from a Raman study of Cl_2 dissolved in carbon tetrachloride [47]. We have confirmed this assignment in our laboratory by obtaining the resonance Raman spectrum of Cl_2 dissolved in CCl_4. The Cl_2 observed in Fig. 2 is most likely a photoproduct of ClOCl or ClClO; however, it may also be unreacted chlorine from the synthesis. A quantitative determination of the amount of unreacted Cl_2 by vis-UV absorption is difficult due to the presence of the much stronger absorption band of ClOCl that significantly overlaps the Cl_2 absorption. It should be noted that this transition was not observed in the resonance Raman spectrum of ClOCl at low intensities, consistent with Cl_2 being a photoproduct.

3.3. Photochemistry

In order to study the photochemistry of Cl_2O in solution, studies of the power dependence of the Raman scattering of Cl_2O as well as the ClO and ClClO photoproducts were performed. The temporal width of the Nd : YAG pulses is 5 ns (full-width at half maximum); therefore, the resonance Raman spectra represent the production and/or decay of Cl_2O, ClO, and ClClO integrated over the temporal duration of the incident laser pulse. The power dependence of the Cl_2O resonance Raman spectrum is presented in Fig. 3. Fig. 3(A) presents a spectrum obtained employing a pulse energy of 57 μJ, the highest actinic energy employed. Fig. 3(B) presents a spectrum obtained using a pulse energy of 6.7 μJ, the lowest actinic energy employed. In both spectra, scattering from Cl_2O, ClO, and ClClO is evident; however, scattering from the ClO and ClClO photoproducts is more intense in the high-energy spectrum. This increase in photoproduct scattering intensity is illustrated by the difference spectrum presented in Fig. 3(C). This spectrum was constructed by subtracting the low-pulse-energy spectrum (Fig. 3(B)) from the high-pulse-energy spectrum (Fig. 3(A)) until scattering corresponding to ClOCl is removed. This

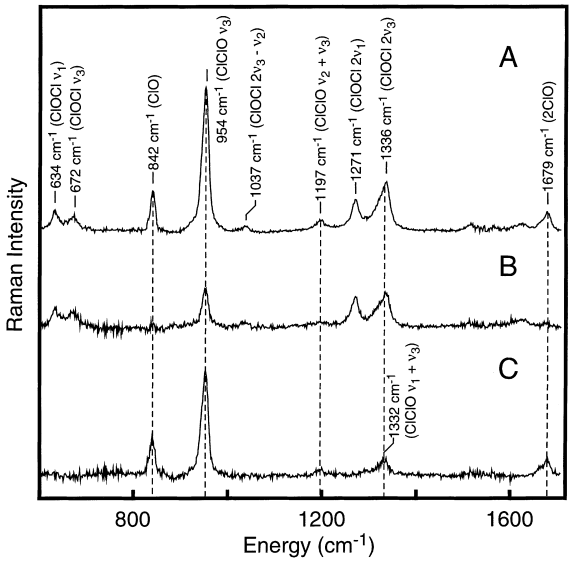

Fig. 3. (A) Resonance Raman spectrum of Cl_2O obtained with 57 μJ/pulse at 282.4 nm. Scattering due to Cl_2O, ClO, and ClClO is observed. (B) Resonance Raman spectrum of Cl_2O obtained with 6.7 μJ/pulse at 282.4 nm. Note that scattering due to Cl_2O is still evident while scattering due to ClO and ClClO is diminished with a reduction in pulse energy. (C) Difference spectrum generated by subtracting the spectrum in (B) from that in (A) until transitions due to Cl_2O are removed. This spectrum demonstrates that ClO and ClClO are photoproducts of Cl_2O. Scattering due to the CCl_4 solvent has been subtracted.

figure clearly shows that with an increase in pulse energy, scattering from the ClO and ClClO photoproducts increases.

The dependence of the resonance Raman scattering on pulse energy (Fig. 3) was used to explore the power dependence of photoproduct formation as shown in Fig. 4. Fig. 4(A) presents the dependence of the Cl_2O scattering intensity on pulse energy. An initial increase in excitation energy results in a linear increase in Cl_2O scattering intensity, but at higher incident energies the scattering intensity increases in a sublinear fashion. Resonance Raman spectroscopy of photolabile molecules has been a challenging pursuit for precisely the reason illustrated by Fig. 4(A); the field used to generate Raman intensity can also result in photoalteration of the sample. The extent of photoconversion can be quantified using the expression for photoalteration by a pulsed excitation [48]. For a photolabile species, the fraction (F) of the species that undergoes photoalteration during illumination from a pulsed source is given by:

$$F = 1 - \exp(-I\sigma\phi) \quad (1)$$

where I is the light intensity (photons/cm^2), ϕ the photoalteration quantum yield, and σ the absorption cross section (cm^2). The above expression demonstrates that, as the incident light intensity increases, the fraction of molecules undergoing photoalteration should also increase resulting in a reduction in scattered intensity for the photolabile species. The plot of Cl_2O resonance Raman intensity as a function of pulse energy is consistent with this expectation (Fig. 4(A)),

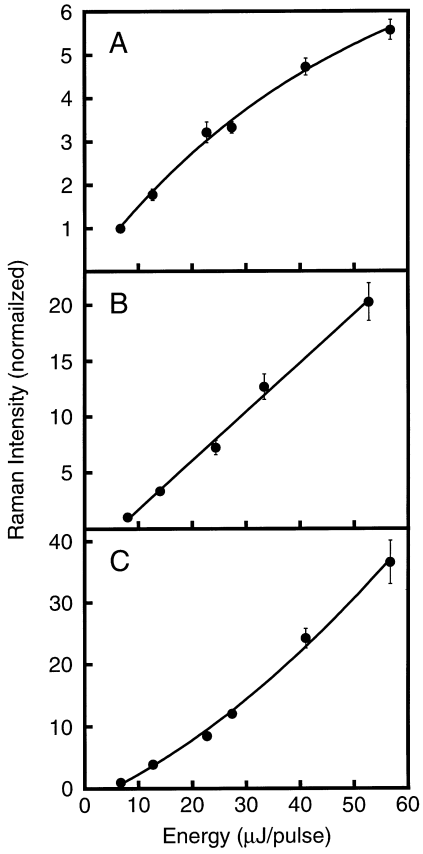

Fig. 4. (A) Dependence of Cl_2O scattering intensity on incident pulse energy. Values correspond to the integrated intensity of the ν_1 and ν_3 bands at 634 and 672 cm^{-1}, respectively. (B) Dependence of ClClO scattering intensity on incident pulse energy. Values correspond to the integrated intensity of the ν_3 transition located at 954 cm^{-1}. (C) Dependence of the ClO scattering intensity on incident pulse energy. Values correspond to the integrated intensity of the 842 cm^{-1} transition. The intensities for a given species were normalized to the intensity observed at lowest energy.

and the data were fit to a modified version of Eq. (1):

$$\text{Intensity} = M[1 - \exp(-0.2\ \mu J^{-1} \times E_{\text{pulse}})] \quad (2)$$

The above equation is obtained from Eq. (1) by setting $\phi = 1$ (all excitation results in photoalteration) and $\sigma = 1.7 \times 10^{-18}$ cm^2 (Fig. 1). The addition of the multiplicative factor M in Eq. (2) simply represents the normalization factor used to scale the fit to the intensities presented in Fig. 4(A). Best fit of Eq. (2) to the data results in $M = 8.28$, with $R = 0.99727$ demonstrating that the sub-linear increase in Cl_2O scattering intensity at large excitation energies is consistent with the onset of photoalteration.

Fig. 4(B) presents the resonance Raman scattering of ClClO as a function of pulse energy. Best fit to the data was obtained with a straight line (intensity = $0.4386\ \mu J^{-1} \times E_{\text{pulse}} - 2.723$, $R = 0.99748$) demonstrating that the photoproduct is a single-photon product of Cl_2O. Two photochemical models can be envisioned that give rise to this behavior. First, ClClO could be produced by the direct photoisomerization of Cl_2O as follows:

$$\text{ClOCl} \xrightarrow{h\nu} \text{ClClO} \quad (3)$$

As discussed above, studies of OClO photochemistry in solution have demonstrated that geminate recombination of the primary photofragments can be efficient. Therefore, ClClO may result from the geminate recombination of the primary ClO and Cl photofragments:

$$\text{ClOCl} \xrightarrow{h\nu} \text{ClO} + \text{Cl} \xrightarrow{gr} \text{ClClO} \quad (4)$$

Both possibilities will be explored in the discussion. Fig. 4(C) displays the resonance Raman scattering of ClO vs. pulse energy. These data are more complex than those of Cl_2O or ClClO. Specifically, at low-pulse energies, the increase in ClO scattering is linear, but at higher pulse energies a quadratic increase in scattered intensity is observed. Best fit to the data was obtained by a sum of linear and quadratic terms (intensity = $0.3922\ \mu J^{-1} \times E_{\text{pulse}} + 0.0005279\ \mu J^{-2}(E_{\text{pulse}})^2 - 2.132$, ($R = 0.9981$). For comparison, a simple linear fit resulted in $R = 0.8981$. This complex dependence suggests that the production of ClO is due to two processes, one where ClO is a primary photoproduct of Cl_2O, and a second process that is dependent on subsequent reactivity. One model consistent with this behavior is:

$$\text{Step 1(a)} \quad \text{ClOCl} \xrightarrow{h\nu} \text{ClO} + \text{Cl} \quad (5)$$

$$\text{Step 2(a)} \quad \text{ClOCl} \xrightarrow{h\nu} \text{ClClO} \quad (6)$$

$$\text{Step 2(b)} \quad \text{ClClO} \xrightarrow{h\nu} \text{ClO} + \text{Cl} \quad (7)$$

In the above scheme, ClO is directly produced by photolysis of Cl_2O with this step dominating at low pulse energies (Step 1). At higher energies, production of ClO can occur through the photolysis of ClClO, such that the production of ClO via this mechanism would be two-photon dependent and, thus, vary quadratically with actinic energy (Step 2). The sum of these two steps results in the photochemical production of ClO that demonstrates both linear and quadratic energy dependence. In summary, two photoproducts of Cl_2O are observed in solution, ClClO and ClO. The photoproduction of ClClO proceeds linearly with actinic energy, and ClO is produced with both linear and quadratic actinic energy dependence.

4. Discussion

The results presented here demonstrate the utility of resonance Raman spectroscopy in monitoring photoproduct formation dynamics. It is interesting to compare the pattern of reactivity observed here to the gas-phase photoproduct formation dynamics of Cl_2O. Recent studies by Okumura et al. [6,7] have demonstrated that photolysis of gas-phase Cl_2O at 308 nm results only in the production of ClO + Cl. This photoproduct channel remains dominant with a decrease in actinic wavelength to 248 nm. Fission of ClO to give Cl and

$O(^3P)$ was also observed at this wavelength, presumably due to the increase in internal energy of the ClO photofragment with an increase in actinic pulse energy. A further decrease in actinic wavelength to 193 nm resulted in the appearance of a second photoproduct channel, $Cl_2 + O(^3P)$. The appearance of this channel was assigned as resulting from excitation into a different electronic transition leading to Cl_2 formation [6]. The appearance of ClO in solution is consistent with the gas-phase reaction dynamics. However, no evidence for production of ClClO in the gas-phase has been reported in contrast to the production of this species in solution.

One possible explanation for the presence of ClClO in solution is that this species is produced by photoisomerization of Cl_2O. Johnsson et al. [27] have suggested that, in low-temperature matrices, the production of ClClO proceeds through Cl_2O photoisomerization. The evidence for a photoisomerization channel leading to ClClO formation included the absence of ClO production, and the observation that Cl_2O and ClClO reach a photostationary state under irradiation at 320–428 nm. A few recent theoretical studies have explored the possibility of Cl_2O photoisomerization [37,49,50]. In particular, the recent study of Chaquin et al. [49] established that ClClO is 18 kcal/mol higher in energy than Cl_2O, with a barrier of 25 kcal/mol existing along the ground-state photoisomerization reaction coordinate. The authors suggested that Cl_2O may also photoisomerize to form ClClO. Finally, a recent theoretical and experimental study on the photoisomerization of dibromine monoxide (Br_2O) found that photoisomerization of Br_2O to BrBrO can occur at higher actinic energies [51]. In short, there is sufficient evidence to suggest that Cl_2O can photoisomerize, resulting in the formation of ClClO.

The dominance of the ClO and Cl photochemical channel in the gas phase suggests that rather than photoisomerization, ClClO may be formed by geminate recombination of the primary ClO and Cl photofragments. This interpretation is consistent with low-temperature matrix studies of Rochkind and Pimentel [21], where the formation of ClClO and the ClO dimer was observed. Chi and Andrews [28] also studied matrix-isolated Cl_2O and found that, following broadband excitation from 220–360 nm, the ClO dimer, ClClO, ClO, and Cl_2 are formed. The recombination of ClO and Cl to form ClClO is reminiscent of the condensed-phase reaction dynamics of OClO; however, recombination of the primary OClO photofragments results in the reformation of OClO and not ClOO. This comparison suggests that if geminate recombination is responsible for ClClO formation, the recombination dynamics are significantly different between OClO and Cl_2O.

Finally, we have also observed the formation of ClO, which is most likely a photodissociation product of Cl_2O in agreement with the gas-phase studies. However, the quadratic dependence of ClO formation on actinic pulse energies suggests that photoexcitation of ClClO also results in ClO formation. The existence of ClO stable on the 5 ns time scale suggests that, if geminate recombination of the ClO and Cl fragments occurs, this recombination is not complete and the fragments have a finite possibility of escaping the solvent cage. Weakly associating solvents, such as CCl_4, are labile to primary photoproduct cage escape so that incomplete geminate recombination would not be unexpected [52]. Therefore, the combined observation of ClO, ClClO, and the power-dependent formation of these species suggests that geminate recombination of the ClO and Cl fragments is primarily responsible for the formation of ClClO. However, the resonance Raman experiments described here lack the time resolution necessary to resolve the dynamics of ClClO formation. To differentiate between the geminate recombination and photoisomerization pathways, we have initiated a femtosecond pump-probe and time-resolved resonance Raman study of Cl_2O photochemistry. The results of this work will appear shortly.

5. Conclusions

We have presented a resonance Raman study of Cl_2O photochemistry in CCl_4. The power-dependence of the resonance Raman spectra demonstrated that photoexcitation of Cl_2O at 282.4 nm results in the formation of both, ClO and ClClO. Given the dominance of the ClO + Cl photochemical channel in the gas phase, it is suggested that the formation of ClClO is due to geminate recombination of the primary ClO and Cl photofragments. Finally, the existence of the stable ClClO isomer should be contrasted with the photochemical behavior of OClO, where the analogous ClOO isomer is not produced. This behavior suggests that although geminate recombination may be a characteristic feature of halo-oxide chemistry in condensed environments, the recombination dynamics are markedly different.

Acknowledgements

The authors would like to thank Margaret Chaffee for her assistance in the preparation of Cl_2O, and acknowledge her support by the National Science Foundation REU program. The National Science Foundation is also acknowledged for their support of this work through the CAREER program (CHE-9701717). Acknowledgment is made to the donors of the Petroleum Research Fund, administered by the American Chemical Society. K.W. Rousslang was supported by a summer research fellowship from the Petroleum Research Fund, and their support through this program is gratefully acknowledged. P.J. Reid is a Cottrell Fellow of the Research Corporation and an Alfred P. Sloan Fellow.

References

[1] F.S. Rowland, Annu. Rev. Phys. Chem. 42 (1991) 731.
[2] J.B. Renard, M. Pirre, C. Robert, D. Huguenin, J. Geophys. Res. 103 (1998) 25383.

[3] S. Solomon, S. Borrmann, R.R. Garcia, R. Portmann, L. Thomason, L.R. Poole, D. Winker, M.P. McCormick, J. Geophys. Res. 102 (1997) 21411.
[4] H.A. Donsig, D. Herridge, J.C. Vickerman, J. Phys. Chem. A. 102 (1998) 2302.
[5] V. Vaida, J.D. Simon, Science 268 (1995) 1443.
[6] C.M. Nelson, T.A. Moore, M. Okumura, T.K. Minton, J. Chem. Phys. 100 (1994) 8055.
[7] T.A. Moore, M. Okumura, T.K. Minton, J. Chem. Phys. 107 (1997) 3337.
[8] Y. Tanaka, M. Kawasaki, Y. Matsumi, H. Fujiwara, T. Ishiwata, L.J. Rogers, R.N. Dixon, M.N.R. Ashfold, J. Chem. Phys. 109 (1998) 1315.
[9] S.P. Sander, R.R. Friedl, J. Phys. Chem. 93 (1989) 4764.
[10] S.L. Nickolaisen, C.E. Miller, S.P. Sander, M.R. Hand, I.H. Williams, J.S. Francisco, J. Chem. Phys. 104 (1996) 2857.
[11] A.W. Miziolek, M.J. Molina, J. Phys. Chem. 82 (1978) 1769.
[12] H.-D. Knauth, H. Alberti, H. Clausen, J. Phys. Chem. 83 (1979) 1604.
[13] A. Esposito, C. Foster, R. Beckman, P.J. Reid, J. Phys. Chem. A 101 (1997) 5309.
[14] C.E. Foster, P.J. Reid, J. Phys. Chem. A 102 (1998) 3541.
[15] J. Thørgersen, P.U. Jepsen, C.L. Thomsen, J.A. Poulsen, J.R. Byberg, S.R. Keiding, J. Phys. Chem. 101 (1997) 3317.
[16] J. Thørgersen, C.L. Thomsen, J.A. Poulsen, S.R. Keiding, J. Phys. Chem. 108 (1998) 8461.
[17] M.J. Philpott, S. Charalambous, P.J. Reid, Chem. Phys. Lett. 281 (1997) 1.
[18] M.J. Philpott, S. Charalambous, P.J. Reid, Chem. Phys. 236 (1998) 207.
[19] S.C. Hayes, M.J. Philpott, P.J. Reid, J. Chem. Phys. 109 (1998) 2596.
[20] S.C. Hayes, M.P. Philpott, S.G. Mayer, P.J. Reid, J. Phys. Chem. A 103 (1999) 5534
[21] M.M. Rochkind, G.C. Pimentel, J. Chem. Phys. 46 (1967) 4481.
[22] A. Arkell, I. Schwager, J. Am. Chem. Soc. 89 (1967) 5999.
[23] C.J. Pursell, J. Conyers, P. Alapat, R. Parveen, J. Phys. Chem. 99 (1995) 10433.
[24] F.H.C. Edgecombe, R.G.W. Norrish, B.A. Thrush, Proc. Roy. Soc. (London) A243 (1957) 455.
[25] N. Basco, S.K. Dogra, Proc. Roy. Soc. Lond. A. 323 (1971) 401.
[26] A.I. Chichinin, Chem. Phys. Lett. 209 (1993) 459.
[27] K. Johnsson, A. Engdahl, B. Nelander, J. Phys. Chem. 99 (1995) 3965.
[28] F.K. Chi, L. Andrews, J. Phys. Chem. 77 (1973) 3062.
[29] M.P. Gane, N.A. Williams, J.R. Sodeau, J. Chem. Soc. Faraday Trans. 93 (1997) 2747.
[30] R.G. Dickenson, C.E.P. Jeffreys, J. Am. Chem. Soc. 52 (1930) 4288.
[31] G.H. Cady, Inorg. Syntheses 5 (1957) 156.
[32] M. Anbar, I. Dostrovsky, J. Chem. Soc. (1954) 1105.
[33] M.M. Rochkind, G.C. Pimentel, J. Chem. Phys. 42 (1965) 1361.
[34] C.-L. Lin, J. Chem. Eng. Data 21 (1976) 411.
[35] D.J. Gardiner, J. Molec. Spect. 38 (1971) 476.
[36] Y. Xu, A.R.W. McKellar, J.B. Burkholder, J.J. Orlando, J. Molec. Spect. 175 (1996) 68.
[37] A. Beltrán, J. Andrés, S. Noury, B. Silvi, J. Phys. Chem. A 103 (1999) 3078.
[38] P. Chaquin, M. Bahou, A. Schriver, L. Schriver, Chem. Phys. Lett. 256 (1996) 609.
[39] J.E. Del Bene, J.D. Watts, R.J. Bartlett, Chem. Phys. Lett. 246 (1995) 541.
[40] T.J. Lee, J. Phys. Chem. 98 (1994) 3697.
[41] M. Nakata, M. Sugie, H. Takeo, C. Matsumura, F. Tsutomu, K. Kuchitsu, J. Molec. Spect. 86 (1981) 241.
[42] A.E. Johnson, A.B. Myers, J. Chem. Phys. 102 (1995) 3519.
[43] M.S. Churio, M.A. Brusa, L.J. Perissinotti, E. Ghibaudi, M.E.J. Coronel, A.J. Colussi, Chem. Phys. Lett. 232 (1995) 237.
[44] U.K. Kläning, T. Wolff, Ber. Bunsenges. Phys. Chem. 89 (1985) 243.
[45] J.S. Margolis, R.T. Menzies, E.D. Hinkley, Appl. Optics 17 (1978) 1680.
[46] R.S. Rogowski, C.H. Bair, W.R. Wade, J.M. Hoell, G.E. Copeland, Appl. Optics 17 (1978) 1301.
[47] W. Holzer, W.F. Murphy, H.J. Bernstein, J. Chem. Phys. 52 (1970) 399.
[48] A.B. Myers, R.A. Mathies, in: T.G. Spiro (Ed.), Biological Applications of Raman Spectroscopy, vol. 2 — Resonance Raman Spectra of Polyenes and Aromatics, Wiley, New York, 1987, pp. 1–58.
[49] P. Chaquin, M.E. Alikhani, M. Bahou, L. Schriver-Mazzouli, A. Schriver, J. Phys. Chem. A 102 (1998) 8222.
[50] R.P. Thorn Jr., L.J. Stief, S.-C. Kuo, R.B. Klenn, J. Phys. Chem. 100 (1996) 14178.
[51] J. Kölm, O. Schrems, P. Beichert, J. Phys. Chem. A 102 (1998) 1083.
[52] P.K. Walhout, J.C. Alfano, K.A.M. Thakur, P.F. Barbara, J. Phys. Chem. 99 (1995) 7568.